Journal of Geophysical Research: Atmospheres

RESEARCH ARTICLE
10.1029/2018JD029272

Observationally Weak TGFs in the RHESSI Data

K. H. Albrechtsen[1], N. Østgaard[1], N. Berge[2], and T. Gjesteland[3]

[1]Birkeland Centre for Space Science, Department of Physics and Technology, University of Bergen, Bergen, Norway, [2]LPC2E, CNRS, University of Orleans, Orleans, France, [3]Department of Engineering Science, University of Agder, Grimstad, Norway

Key Points:
- We show that there is a fluence distribution of TGFs down to 0.22 of the detection threshold, and we do not see a cutoff in the RHESSI TGF distribution
- We find that there are six times as many TGFs inside of RHESSI's field of view, than can be identified by current search algorithms
- We find that observationally weak TGFs largely originate at larger radial distances and higher latitudes from the subsatellite point

Supporting Information:
- Text S1
- Text S2

Correspondence to:
K. H. Albrechtsen,
kjetil.albrechtsen@uib.no

Citation:
Albrechtsen, K. H., Østgaard, N., Berge, N., & Gjesteland, T. (2019). Observationally weak TGFs in the RHESSI data. *Journal of Geophysical Research Atmospheres*, *124*, 287–298. https://doi.org/10.1029/2018JD029272

Received 29 JUN 2018
Accepted 22 NOV 2018
Accepted article online 29 NOV 2018
Published online 11 JAN 2019

Abstract Terrestrial gamma ray flashes (TGFs) are sub-millisecond bursts of high energetic gamma radiation associated with intracloud flashes in thunderstorms. In this paper we use the simultaneity of lightning detections by World Wide Lightning Location Network to find TGFs in the Reuven Ramaty High Energy Solar Spectroscopic Imager (RHESSI) data that are too faint to be identified by standard search algorithms. A similar approach has been used in an earlier paper, but here we expand the data set to include all years of RHESSI + World Wide Lightning Location Network data and show that there is a population of observationally weak TGFs all the way down to 0.22 of the RHESSI detection threshold (three counts in the detector). One should note that the majority of these are "normal" TGFs that are produced further away from the subsatellite point (and experience a $1/r^2$ effect) or produced at higher latitudes with a lower tropopause and thus experience increased atmospheric attenuation. This supports the idea that the TGF production rate is higher than currently reported. We also show that compared to lightning flashes, TGFs are more partial to ocean and coastal regions than over land.

1. Introduction

Terrestrial gamma ray flashes (TGFs) are sub-millisecond bursts of high-energy gamma radiation and are the product of the bremsstrahlung process from relativistic electrons accelerated upward by the high electric fields in thunderstorm clouds, associated with intracloud (IC) lightning. The process produces a number of electrons typically in the order of 10^{17}–10^{19}, which again produce a comparable number of photons (Dwyer & Smith, 2005; Gjesteland et al., 2015; Mailyan et al., 2016).

+TGFs are the most energetic natural occurring photon phenomena in our atmosphere with photon energies up to ~40 MeV (Marisaldi et al., 2010), and it may follow that they have the ability to contribute to a significant energy deposition in the atmosphere. However, this is dependant on how frequently they occur; are they a rare phenomenon or a common occurrence? Although improvements have been made in understanding this phenomenon in recent years, there are still a lot of unknowns associated with TGFs.

The first detection of a TGF was obtained in 1991 with the Burst and Transient Source Experiment (BATSE), a NaI detector onboard the Compton Gamma-ray Observatory. BATSE's primary mission was to investigate astrophysical gamma ray bursts, a phenomenon with a much longer time scale than TGFs. However, the BATSE instrument managed to detect 12 TGFs in the first 2 years of its operation (Fishman et al., 1994). BATSE's total time of operation was 9 years, and it identified 78 TGFs during that time.

In 2002 the satellite Reuven Ramaty High Energy Solar Spectroscopic Imager (RHESSI) was launched, and despite that its primary mission is to study solar flares (Smith et al., 2002), its instrument is also able to detect TGFs. RHESSI consists of nine high resolution Germanium detectors (Smith et al., 2002). Although having a smaller effective area for a typical TGF spectrum than BATSE, 239 cm^2 versus 2,025 cm^2, RHESSI has the ability to telemeter raw count data to ground where the data can be analyzed by search algorithms (Dwyer et al., 2012; Grefenstette et al., 2008). In 2009, Grefenstette et al. (2009) published the details of the first search algorithm performed on the raw RHESSI data. Using data between March 2002 and February 2008 they identified 820 TGFs, far more than BATSE did in its lifetime. In 2012, Gjesteland et al. (2012) presented another search algorithm for the RHESSI data that more than doubled the number of identified TGFs. This was partly due to the original search algorithm being deliberately conservative to get a clean (i.e., low number of false positives) data set, as well as Gjesteland et al. (2012)'s more accurate use of Poisson statistics.

Other notable satellites include the Italian satellite Astrorivelatore Gamma a Immagini LEggaro (AGILE), which orbits the Earth with a very small inclination of 2.5°, spending the majority of its time around equator, where there is a very high lightning incidence. Launched in 2007, and with its original trigger configuration, AGILE detected a total of 32 events in its first 9 months of operation, or approximately four per month (Marisaldi et al., 2010). After a change in their trigger logic in March 2009, this almost doubled to approximately eight events per month (Marisaldi et al., 2010). In 2015 the AGILE team removed the veto system for the anticoincidence shield and thereby increased their TGF detection rate by almost an order of magnitude (Marisaldi et al., 2015).

In addition, the Fermi satellite's Gamma-ray Burst Monitor (GBM) is also used for TGF studies. Fermi was launched on 11 July 2008, and the GBM is a trigger instrument similar to BATSE, but with a 16-ms trigger time instead of BATSE's 64 ms. In its first year, GBM triggered on 12 TGFs (Briggs et al., 2010). Until 10 November 2009, GBM only used data from their NaI detectors to trigger the instrument. By changing their trigger algorithm to include data from the bismuth germanate scintillators, which detect a much harder energy spectrum, the trigger rate increased by a factor of ∼8, from 1 every fourth week to about 2 per week (Fishman et al., 2011).

From 9 July 2009 a new data mode was introduced by the Fermi team where certain geographical areas with a high incidence of lightning (and TGF production) would be subject to continuous telemetry. The implementation of the continuous time tagged event data mode and its subsequent offline TGF search have increased the detection rate of TGFs about tenfold (Briggs et al., 2013). After November 2012 the Fermi team implemented this change for the entire orbit, detecting ∼800 TGFs per year (Roberts et al., 2018).

One should note that the Airborne Detector for Energetic Lightning Emission (ADELE) passed by 1,213 lightning discharges within a 10-km horizontal distance (mostly flying at an ∼14-km altitude) and detected only one TGF (Smith et al.,2011; it also passed 200 discharges within 4 km without detecting any TGF). Due to the singular TGF found by ADELE, Smith et al. (2011) argued that the TGF-to-flash ratio would be in the order of 10^{-2} to 10^{-3}. However, Østgaard et al. (2012) argued that based on RHESSI, Fermi, and ADELE measurements, one could not rule out that all lightning produce TGFs.

The most recent instrumentation include the Atmosphere-Space Interactions Monitor instrument. Atmosphere-Space Interactions Monitor was successfully launched in April 2018.

The general trend we are highlighting is that with more sophisticated search algorithms and better detectors, the TGFs detection and identification rates have been ever increasing. This begs the question: How frequent are TGFs?

In 2015, Østgaard et al. (2015) presented a method to further increase the detected frequency of TGFs in RHESSI data. By using the simultaneity of World Wide Lightning Location Network (WWLLN) detections and TGFs, they evaluated RHESSI data for every WWLLN detected lightning flash inside RHESSI's field of view (FOV). They found evidence that there exists a population of TGFs that is too faint at satellite altitude to be identified as TGFs by the current search algorithms. By performing a statistical analysis of RHESSI lightcuves in 2006 and 2012 at the time of lightning, taking into account the systematic delay of the RHESSI clock and the travel time from thundercloud tops to RHESSI's position, they found a significant signal above the noise level, indicating a population of weak TGFs. These weak TGFs are either intrinsically weak, or appearing weak in the detector due to attenuation from traveling through the atmosphere, or by being very brief in time, so that they suffers significant deadtime effects.

By fitting a power law to the data they found a fluence distribution with a power of $\lambda = 1.85$ close to the roll-off index of 1.7 as suggested by Østgaard et al. (2012). However, they noted that these have not been deadtime corrected and that during the later stage of the RHESSI mission the instrument has been heavily degraded.

Smith et al. (2016) made an extended analysis of weak TGFs by using WWLLN data. Using RHESSI data from 1 January 2004 till 31 December 2012, they found a large statistical increase in gamma rays; however, their average level of gamma ray emission per lightning discharge is fairly low, estimating that less than 1% of lightning flashes produce TGFs.

In this paper we will extend the data set presented in Østgaard et al. (2015) for all years between 2002 and 2015 and investigate the TGFs' conformity to a power law fluence distribution after being deadtime corrected. Knowing the locations of TGF production, we also investigate in what areas the TGFs are detected, specifically looking at land/coast/ocean.

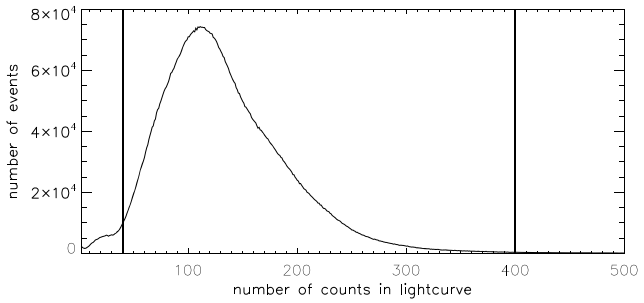

Figure 1. A histogram of the number of total counts in the 100-ms datastrings corresponding with World Wide Lightning Location Network detections. The vertical black lines represent the cutoff of events we discard.

2. Data and Method

It is currently believed that the TGF and Very Long Frequency (VLF) signals are both produced during the propagation of the positive leader, moving between the main negative and upper positive charge center in a positive IC flash (Shao et al., 2010). It is currently undetermined if a TGF is produced just before, after, or simultaneous with the VLF signal, and the exact mechanism by which it is produced is unknown. It has been suggested by Connaughton et al. (2013) and Dwyer and Cummer (2013) that the TGFs themselves can produce the VLF signal, and in other cases the VLF signal is produced by related IC lightning strokes. The precise nature of this relationship is not addressed in this study, as we merely exploit the fact that they occur nearly simultaneously (Connaughton et al., 2010, found Fermi TGF-WWLLN pairs to be simultaneous to ∼40 μs). We use the World Wide Lightning Location Network (WWLLN) for lightning location and use data from August 2002 to December 2015.

WWLLN was reported to have a detection efficiency of 3.88% for cloud-to-ground (CG) and 1.78% for IC flashes in 2006–2007, and for 2008–2009 this increased to 10.30% and 4.82%, respectively (Abarca et al., 2010). Rudlosky and Shea (2013) reported the detection efficiency for IC and CG combined to be ∼10% in 2012 and also pointed out that the detection efficiency is strongly dependent on geographical position. It also depends on the strength of the flash, as Mallick et al. (2014) estimated that the detection efficiency is ∼30% for flashes of 30 kA. If we assume that WWLLN has a 2:1 preference for detecting CG lightning and that ∼75% of all flashes are of the IC type (Boccippio et al., 2001), we can say that 3/5 WWLLN flashes in our data set are IC lightning, and the remaining 2/5 represents CG flashes. As we do not expect any CG flash to be associated with any counts in RHESSI, these datastrings will merely increase our background level.

As a rough search we evaluate every WWLLN detection in relation to RHESSI's position and reject every flash that occurs outside a 1,000-km radius from RHESSI's footpoint, as it would seem unlikely that any TGF produced that far from the subsatellite point would give a detectable signal in the instrument. In addition, including events that far would most likely only contribute with more RHESSI background counts. For each lightning detection we extract a 100-ms interval of data from RHESSI (±50 ms centered around the lightning detection), which we refer to as datastrings.

Our assumption is that each of these lightning flashes could hypothetically produce a TGF, and for each detection we take into account the travel time from their location and altitude (assumed to be 15 km for each lightning flash) to the position of RHESSI. We also correct for the clock error on RHESSI's internal clock. This clock error is a constant offset that needs to be corrected, but on two separate occasions the offset has changed due to updates in the RHESSI software. Mezentsev et al. (2016) did an analysis and found that between RHESSI's launch date and 5 August 2005 the offset was −2,359 ± 101 μs. From 5 August 2005 to 21 October 2013 it was −1,808 ± 50 μs, and from 21 October until the time of writing it is −2,003 ± 57 μs.

We also remove datastrings with unusually high or low background rates. Figure 1 shows the distribution of number of counts in a datastring, and we remove events with less than 50 counts and more than 400 counts in the 100-ms interval. This is to remove events where RHESSI is turned off due to transit over the South Atlantic Anomaly, as well as RHESSI's annealing process. It also removes datastrings that are only partially filled, for example, events where RHESSI turns off/on during the 100-ms interval.

From Figure 1, it is clear that it does not follow a Poisson distribution, as we would expect from the random nature of the events. The distribution we see is much wider, as a Poisson with an average of 110 ms should have a 4σ width of 42 ms. One of the reasons for larger width is the natural variation in background over magnetic latitude as the satellite orbits the earth. Another reason for this effect is the onboard mechanism of RHESSI called decimation. Decimation occurs when RHESSI's onboard memory starts to fill, and the instrument will reject all counts but one out of every N counts below a certain energy E, where N is typically 3 or 4 and E = 150 to 450 keV (Smith et al., 2002). This has tends to shift the peak of Figure 1 to the left.

However, the main reason for this widening is that RHESSI experience radiation damage over time; as time goes on the RHESSI instrument experiences a degradation due to high-energy background. The brief explanation is that high-energy protons (and to a lesser degree neutrons) interact with the germanium detector,

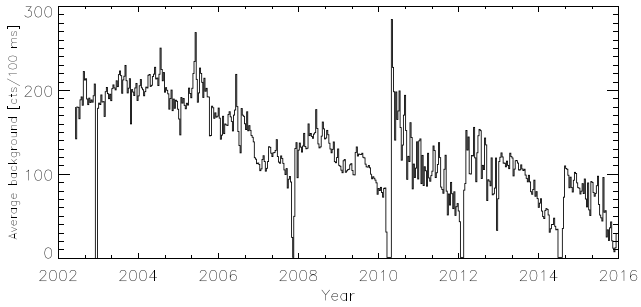

Figure 2. The average number of counts in the collected Reuven Ramaty High Energy Solar Spectroscopic Imager datastrings, binned at 10-day intervals. We see the average count rate decreasing until an anneal is performed (when there are no data), temporarily increasing the sensitivity. The missing data in late 2002 are not due to an anneal, but missing World Wide Lightning Location Network data.

producing defects and disordered regions. These disordered regions can attract and trap holes resulting in a reduced energy measurement, and potentially loss of particle detection (Owens et al., 2007). Over time this degradation shifts the peak in Figure 1 to the left (as RHESSI detects fewer counts). When RHESSI undergoes its annealing process, this again shifts it to the right, as annealing temporarily increases the instrument sensitivity. The change in instrument sensitivity can be seen in Figure 2, and one can see that the average count rate decreases as time passes, and the anneals in 2007, 2010, 2012, and 2014 temporarily restore the sensitivity (the drop in data in 2002 is due to missing WWLLN data).

3. Results

By performing the travel time correction for each WWLLN detection (and taking into account the RHESSI clock error), any potential gamma rays produced with any WWLLN detection should hit the satellite at $t = 0$. By superposing all of these we can find the resultant signal deposited by all detected lightning flashes within RHESSI's FOV. We can test the validity of this approach by using only WWLLN detections occurring within 1 ms of an already identified TGF. This should align all counts from previously identified TGFs at $t = 0$ in a histogram. In Figure 3 we have superposed 383 datastrings where the WWLLN detection occurred within 1 ms of an identified TGF, and we can see that counts from the already identified TGFs fall at $t = 0$ as expected. We use a 250-μs bin, as this is the approximate duration of a typical TGF (Fishman et al., 2011; Gjesteland et al., 2010), and larger than the typical RHESSI clock uncertainty of ~50 μs (~100 μs before 5 August 2005) and the typical WWLLN timing uncertainty of 30–45 μs.

We can use the same method but only include WWLLN detections that are not associated with any identified TGF: by removing all datastrings occurring within ±50 ms of a TGF identified by the Gjesteland et al. (2012) algorithm. This ensures that no known TGFs are included in the datastrings.

We superpose (stack) RHESSI datastrings from 2002 till 2015 that correspond with a WWLLN detection, within a 900-km radius of RHESSI's footpoint, using 250 μs bins, and the result can be seen in Figure 4. Through optimization we found that using a 900 km gave us the best signal-to-noise ratio (in terms of number of sigma of the peak in Figure 4). This plot has all the TGFs found by the Gjesteland algorithm removed. Figure 4 shows a 10.14 σ increase in gamma ray counts above background level at the time of the lightning flash. The sigma, σ, is the statistical variation of background. This indicates that there is a population of unidentified TGFs that has not been identified by current search algorithms. The figure shows an excess of 13,554 counts on top of a mean background of 2.084 million counts from 6.38 million lightning flashes (note that the x-axis does not start at 0). Comparing this to Smith et al. (2016), we see that we get a lower counts/flash ratio, $\sim 2.1 \cdot 10^{-3}$ compared to their $7.43 \cdot 10^{-3}$. This can likely be attributed to the differences in search radius, as we use 900 km versus their 700 km.

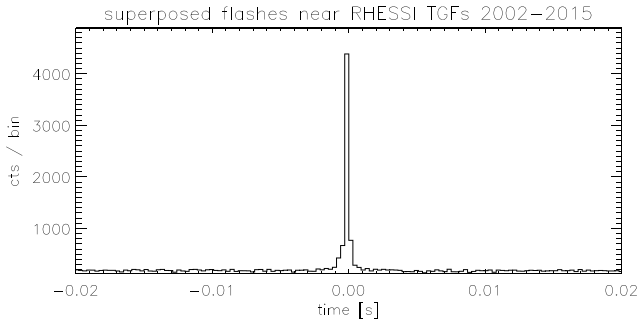

Figure 3. A total of 383 superposed Reuven Ramaty High Energy Solar Spectroscopic Imager (RHESSI) datastrings corresponding to World Wide Lightning Location Network detections occurring within 1 ms of an identified terrestrial gamma ray flash (TGF) in the Gjesteland et al. (2012) catalog, and binned with 250 μs.

This leads to the question: Do we see many low fluence TGFs or fewer, high fluence TGFs? In Figure 5 we show the fluence distribution of the center 250 μs bins versus the fluence distribution of the background. The background is averaged over all bins (excluding the peak bin ± 5 bins). It is clear that from five counts and up there is a notable increase compared to the background level.

Furthermore, we can plot the difference of the count level in Figure 5, meaning the black histogram minus the red histogram, to see the resultant difference of the center bin fluence distribution compared to the background fluence distribution. The result is seen in Figure 6.

In Figure 6 we see a clear population of weak TGFs going all the way down to three counts in the detector (less than this is associated with some very high uncertainties). This corresponds to 0.22 of the effective detection threshold 13.625 (Smith et al., 2016, Appendix A). One should also note that we do not see any signs of a cutoff (nor a steep change) in the TGF distribution, as was presented as possible scenarios by Smith et al. (2016).

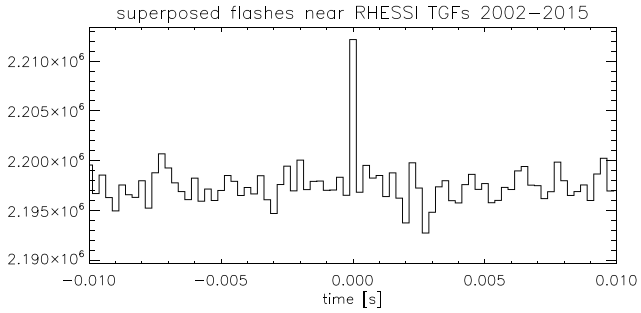

Figure 4. Superposed histogram of RHESSI datastrings centered at $t = 0$. The plot is made by summing the datastrings of 6,375,419 lightning flashes occurring within 900 km of RHESSI's subsatellite point between the years 2002 and 2015 binned at 250 μs. The peak is 10.15 σ over the background level. RHESSI = Reuven Ramaty High Energy Solar Spectroscopic Imager; TGF = terrestrial gamma ray flash.

Summing up all net events from 3 to 20 counts we find ∼2,171 events. Adding this to the number of TGF-WWLLN matches found with the previous search algorithm under the same conditions, 368, we could expect there to be around 2,539 TGFs associated with WWLLN in the RHESSI data. A factor of ∼6 more than TGFs identified by only the search algorithm. If we look at all the TGFs identified in this period by the algorithm outlined in Gjesteland et al. (2012), we find 3,883 TGFs, meaning there could be an additional $2.3 \cdot 10^4$ TGFs originating within the RHESSI FOV, too faint to be identified, but able to deposit at least three counts into the detector. However, this does assume that the brightness distribution of the TGF population that triggers WWLLN is the same as the one that does not, something that is not guaranteed. We can compare this to the total number of lightning flashes we have in RHESSI's FOV during this period, 6,375,419 (same as in Figure 4); however, this number includes both IC flashes and CG flashes. As mentioned in section 2, WWLLN has a higher detection efficiency for CG flashes, but IC flashes are more common, and it follows that ∼60 % of WWLLN detections are IC flashes. Taking the total number of TGFs, $2.7 \cdot 10^4$, divided by $3.83 \cdot 10^6$, we get the fraction of WWLLN detected IC flashes that produce a TGF depositing 3+ counts in RHESSI; $\approx$ 0.0071, less than 1%. Keep in mind that this is with the instrument degradation (seen in Figure 2) and that without it, we would expect to see even more weak TGFs. This is comparable to Smith et al. (2016) where they estimated an upper bound of 1% of IC flashes producing TGFs (although they used data from 2004–2012, and would also have the majority of their data from a degraded RHESSI instrument). Østgaard et al. (2012) estimated a 2% TGF/IC flash ratio by fitting a power law to the fluence distribution of TGFs; however, they pointed out that if the distribution had a roll-off under the RHESSI detection threshold, they could not rule out that all IC flashes produce TGFs (they only used data from before the RHESSI instrument degradation). Briggs et al. (2013) found a ratio of 1:2,600 between TGFs over Fermi GBM's intensity threshold and LIS-detected (Lightning Imager Sensor oboard the Tropical Rainfall Measuring Mission) flashes.

One of the reasons many of these are observed fainter than the search algorithm TGFs is that they originate further away from RHESSI's subsatellite point. Referring to Figure 5, at six or more counts, we can reasonably assume that most of the events are TGFs. We can then take all of these and plot how far away from RHESSI's subsatellite point they were produced and compare it with the TGFs in the second RHESSI catalog that has WWLLN matches. This can be seen in Figure 7. Note that we have divided by the total area of each "shell" in distance to account for bins further away having a larger area. We have also normalized each curve so the area under it is equal to 1. We see that observationally weak TGFs are generally produced further away, meaning that they have to traverse more atmosphere before they reach RHESSI, which could indicate they are "normal fluence" TGFs that experience more attenuation as well as an $1/r^2$ effect. The same conclusion was reached by Smith et al. (2016) and could help explain why McTague et al. (2015) did not see any new TGFs in their study, as they used a search radius of 400 km.

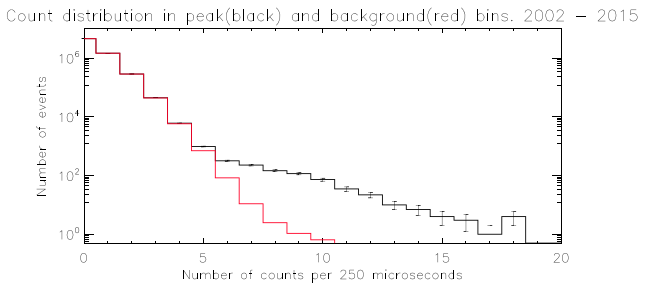

Figure 5. The registered counts by Reuven Ramaty High Energy Solar Spectroscopic Imager in the central 250 μs bin corresponding with the World Wide Lightning Location Network detection (black) and the average background for each of the events (red). From years 2002–2015.

Another point that we would like to make is that we have to keep in mind two different populations of these observationally weak TGFs when referring to Figures 5 and 6. We can see in Figure 6 that we have TGFs down to three counts in the detector, but it would be impossible to actually identify these events. All we can say is that they exist in the data. On the other hand, we see from Figure 5 that above six counts, we have a much lower rate of false positives and we can with some level of certainty claim that these events are real TGFs. For example, above six counts, we have 966 total events, and we expect 100 of these to be false positives based on the background level in Figure 5, about ∼10%. However, above seven counts we have 649 events, and only ∼16 of these would be false positives (∼2.5%). This population above six counts marks not only a population just existing in the data but also a population of observationally weak TGFs where we can identify them with time and location. As part of the

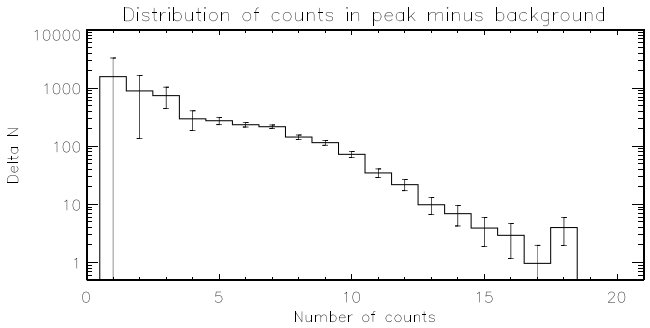

Figure 6. The distribution of counts in the peak bin minus the distribution of the average background.

supplementary material we will upload a list of these, which could be used for further exploration by the community.

3.1. Deadtime Correction And Power Law

It was first suggested by Collier et al. (2011) that the fluence distribution of RHESSI TGFs is a power law of the form $\frac{dN}{dn} \propto n^{-\lambda}$, where N is the number of TGFs with source photon counts of n, and λ is the spectral index. However, the power law must change at lower fluences to avoid a nonphysical number of low fluence TGFs, as we can at most have as many TGFs as lightning flashes. The question then is where does this change or how far down in fluence can we extrapolate this power law. Knowing the slope of the curve, as well as how far back it extends, can give useful information of the production rate of low fluence TGFs.

Several papers have looked into estimating the global production of TGFs rate based on the exponent of a fitted power law (Marisaldi et al., 2014; Østgaard et al., 2012; Tierney et al., 2013) and have found consistent results for the value of the exponent in such a power law, ranging from 2.2 to 2.4. Østgaard et al. (2012) suggested that a power law with a roll-off at lower counts would better fit the data. As our data are mostly in this lower count region, we will perform a fitting procedure to see if the observationally weak TGFs conform to this prediction.

We perform a deadtime correction of our data similar to that presented in Østgaard et al. (2012). We also include TGFs from the search algorithm that have a WWLLN detection, as they are also found with our method and will increase our data set. The main difference (when it comes to deadtime correction) is that we use a maximum likelihood estimation to find the duration of each event, instead of fitting a Gaussian to already binned data. The reasoning is that many of the intrinsically weak TGFs have a very short duration, and pre-binning them would affect the determined duration. As pointed out by Østgaard et al. (2012), RHESSI has a roughly 1:1 relationship between incoming and measured counts up to around 15 counts; however, this is very dependent on the duration of the event, as the same number of particles hitting the detector in a shorter timespan will mean that they are closer together in time. As most of our weak events are brief in time, the observationally weak TGFs are still subject to deadtime.

We take each event with at least six counts within the central 250 μs bin and run the potential TGF through a maximum likelihood estimation to find the best fit of Gaussian, and hence its duration, assumed to be 4 σ of the fit. We then set the event to be of how many counts are detected within that 4 σ (this can in some cases be less than six). We run a Monte Carlo simulation for each event where we randomly distribute counts within the duration of the event, and each of the counts hits a random detector segment. Each simulated event goes

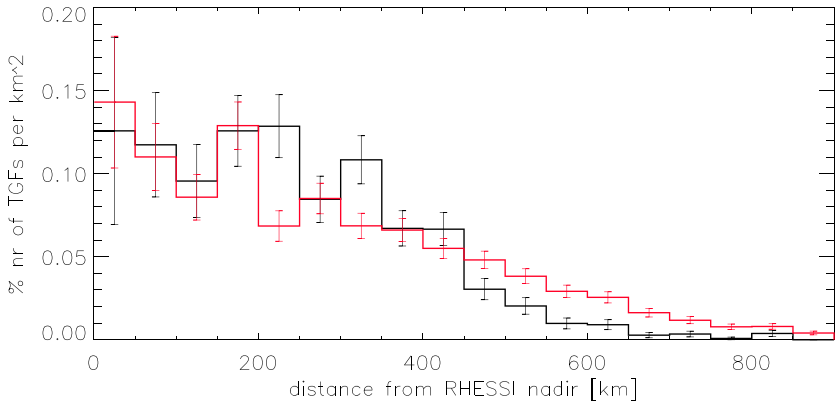

Figure 7. The distance between WWLLN detections and RHESSI's subsatellite point for TGF/WWLLN pairs. The black line represents the second RHESSI catalog with WWLLN matches; the red represents observationally weak TGFs with at least six counts. RHESSI = Reuven Ramaty High Energy Solar Spectroscopic Imager; TGF = terrestrial gamma ray flash; WWLLN = World Wide Lightning Location Network.

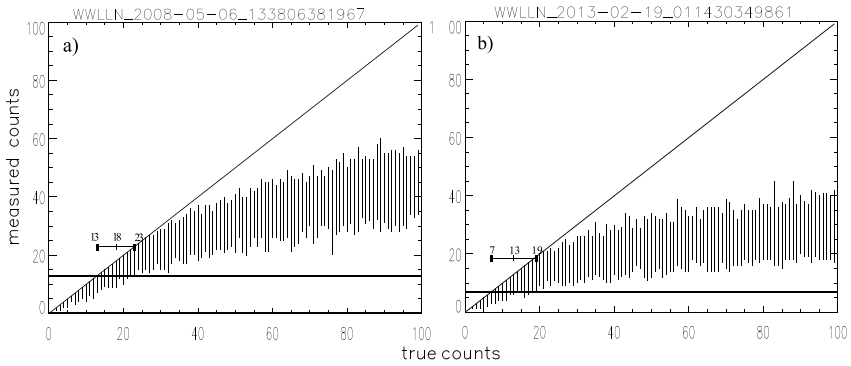

Figure 8. (a) Simulation of the terrestrial gamma ray flash associated with the World Wide Lightning Location Network (WWLLN) flash detected on 6 May 2008 is shown and has a duration of 232 μs. The true fluence counts increase from 0 to 100, and the vertical lines represents the range of counts measured after taking into account deadtime effects. The diagonal line represents a 1:1 relationship. The horizontal black line shows the number of counts detected by RHESSI in this event. Where it intersects with the vertical lines represents the possible number of true counts that produced the measured counts (13). Here we estimate the true event to be 18 ± 5 counts. (b) Simulation for a seven-count event, illustrating that events with a low number of detected counts can have a large number of true counts.

from 0 to 100 incoming counts, and each of these is repeated 100 times to get an average of how many counts are lost due to deadtime effects. Figure 8 shows two examples of a simulation of an event.

We see in Figure 8 that a large range of incoming photons can produce the number of counts we see in an event (represented by the horizontal line). We have taken the middle point of the possible incoming counts to be the incoming count number. This process has to be applied to each event, and each event gets associated with its likely number for incoming counts. Doing so, we can plot how the fluence distribution changes due to deadtime, seen in Figure 9. As expected the graph shifts to the right. The black histogram in Figure 9 should represent the lower fluence end of TGFs discussed in Østgaard et al. (2012). Note that some events in Figure 9 have less than six counts. This is due to some counts being outside the 4 σ duration found from maximum likelihood estimation. In Figure 10 we attempt to fit a single power law to the distribution (black line); however, this distribution also seems to be able to be fitted with another roll-off, shown by the red line. We note that the values obtained from this process is very dependent on where we put the "break," and what range we include in the fit, as the power law exponent is very sensitive to small changes.

However, our data include all data from RHESSI from the years 2002–2015, which includes data after the instrument had suffered degradation. Even though RHESSI has undergone four anneals between 2002 and the end of 2015, the detection threshold has been steadily decreasing, and data from later years are not necessarily compatible with data from earlier years. So to make a better comparison with the work done in Østgaard et al. (2012), we include only data from the same time range. This can be seen in Figure 11 (data from 2002–2005), where we have plotted data between 2002 and the end of 2005, and we can see that there is no apparent roll-off of the power law at lower count rates. Using this limited data set, we only have 181 events, so there

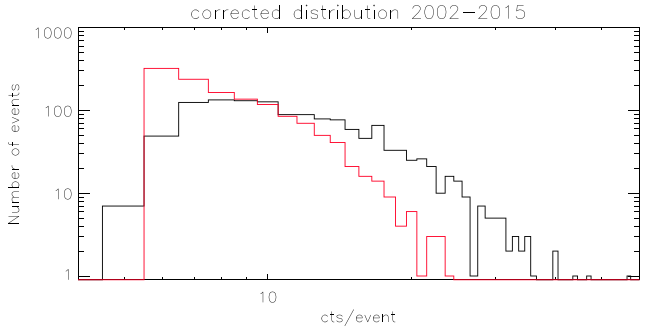

Figure 9. The original fluence distribution (red) compared to the deadtime corrected fluence disrtibution (black). As we can see, many of the events shift to higher fluences. Here we include TGFs from the Gjesteland et al. (2012) algorithm to use all possible TGF + WWLLN events. TGF = terrestrial gamma ray flash; WWLLN = World Wide Lightning Location Network.

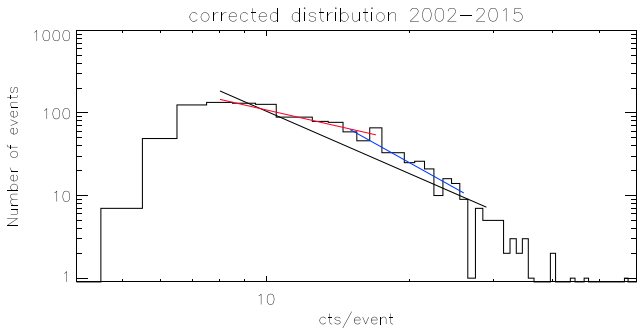

Figure 10. The fluence distribution of deadtime corrected terrestrial gamma ray flashes found by having at least six counts in Reuven Ramaty High Energy Solar Spectroscopic Imager in a 250 μs bin at the time of a World Wide Lightning Location Network detection. Includes all events from 2002 to 2015. The black line represents a power law with exponent $\lambda = 2.5$, the red line $\lambda = 1.3$, and the blue line $\lambda = 3.2$.

might not be enough data to give an adequate answer (Østgaard et al., 2012, had 591 events, but with a 5% match rate with WWLLN at the time, along with a six times increase of observationally weak events, we still only have a third of their number).

This could indicate that accurately fitting a power law to RHESSI data from 2006 onward might not be possible, and due to the changing sensitivity of the RHESSI instrument, consistent data over the years cannot be expected.

3.2. Land-Coastline-Ocean Dependency

Since we now have a large data set of TGFs (both observationally weak and TGFs found by the Gjesteland algorithm), all with WWLLN matches, we can use their location data to investigate if there exists any land/ocean dependence in the TGF data.

It has already been shown that the characteristics of thunderstorms and lightning activity are different over land and over ocean. Examples include phenomena such as differences in flash rates (Christian et al., 2003), differences in the occurrences of Transient Luminous Events (Chen et al., 2008), and differences in storm sizes (Bang & Zipser, 2015). Smith et al. (2010) showed that the TGF/lightning ratio is suppressed inland (over Africa) and enhanced near the coastal regions of Middle America and South East Asia. Splitt et al. (2010) stated that TGF occurrences are more frequent over/near coastlines and large islands and noted that the distribution of RHESSI TGFs correlates well with the global lightning distribution. Roberts et al. (2018) supports this by using Fermi and WWLLN data, showing that TGFs are more common near coastlines.

Exploring whether TGFs follow any land/coastline/ocean patterns could help give information to what kind of processes are associated with them. We have defined a coastal zone of ±150 km from the coastline, taken as the approximate dimension of a cloud system, which should remove any ambiguity in case a storm is partially over ocean and partially on land. Again, we chose to include only WWLLN event that results in six counts in RHESSI at the time of lightning (within a 250-μs bin). A visualization of this can be seen in Figure 12.

As we can see in Table 1, the coastal zones are overrepresented when it comes to TGF production compared to WWLLN detections. It would appear that thunderstorms (or at least WWLLN detections) that occur over ocean or coast (even more so for the coast) are more likely to produce a detectable TGF. We say detectable, as it is unknown if different regions produce TGFs different altitudes. This is consistent with previous work where the geographical region of Congo has a very high lightning incidence, but a lower TGF per lightning ratio compared to the Caribbean and South East Asia, which consist of a lot more ocean and coastline.

Christian et al. (2003) show in their analysis that lightning by itself mainly occurs over land areas, with an average land/ocean ratio of ~10:1. This indicates not only that TGFs themselves are preferential to ocean/coastal storms but also that WWLLN detections are biased toward ocean/coastal detection compared to Christian et al. (2003). Several papers have indicated that CG lightning over ocean achieve higher peak currents (Cooray

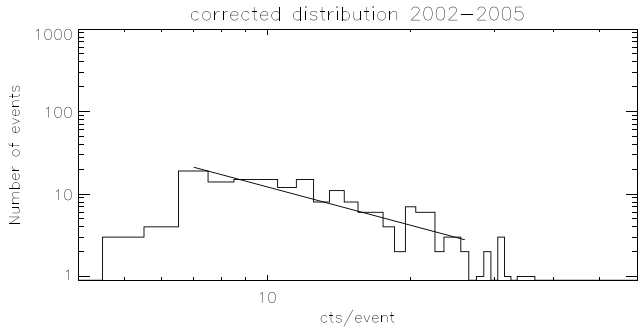

Figure 11. The fluence distribution of deadtime corrected terrestrial gamma ray flashes found by having at least six counts in Reuven Ramaty High Energy Solar Spectroscopic Imager in a 250 μs bin at the time of a World Wide Lightning Location Network detection. Includes all events from 2002 to the end of 2005 (including the terrestrial gamma ray flashes from the Gjesteland et al., 2012, catalog) for a total of 181 datastrings. The black line represents a power law fitting with $\lambda = 1.5$.

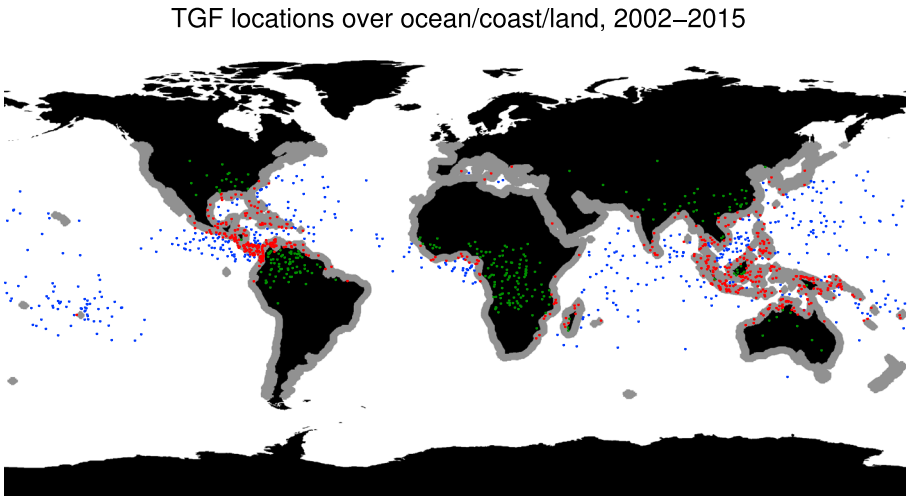

Figure 12. The distribution of TGFs with WWLLN matches on a world map. Blue dots represents TGFs over ocean, red over coast, and and green over land areas. These include both weak TGFs and TGFs from the Gjesteland et al. (2012) catalog with a WWLLN match. TGF = terrestrial gamma ray flash; WWLLN = World Wide Lightning Location Network.

et al., 2014; Nag & Cummins, 2017; Said et al., 2013). The higher peak currents over ocean could indicate that thunderstorms over oceans are able to build up higher potentials before discharging, thus having a greater ability to produce TGFs and stronger sferics (which are detected by WWLLN).

3.3. Latitude Distribution Of Observationally Weak TGFs

Another point to look into is the latitude distribution of observationally weak TGFs to see if they conform to any specific preference. Figure 13 shows the relative number of Gjesteland TGFs compared to the relative number of observationally weak TGFs per latitude. It shows that we are able to detect more TGFs that are produced at higher (absolute) latitudes, compared to those found by the search algorithm.

A reason for this could be the lower altitude of the tropopause at higher latitudes, which again means a lower cloud top. This means that the TGFs would have to propagate through more air to reach RHESSI and thus be attenuated more. This is consistent with the work done in Nisi et al. (2014), where they compared TGFs from the first and second RHESSI catalogs (Gjesteland et al., 2012; Grefenstette et al., 2009). They find that TGFs from the second catalog (and thus generally weaker observationally) have a larger portion originating at higher tropopause pressure (which again translates to a higher absolute latitude, but lower cloud top altitude). This is consistent with Smith et al. (2010) where they find that the majority of their TGFs are strongly biased toward tropopause altitude. Comparing this to our results in Figure 7, it would seem that observationally weak TGFs occur both further away from the RHESSI FOV and at higher latitudes. This could explain why McTague et al. (2015) did not see any population of observationally weak TGFs, as they were searching within a 400-km radius around Fermi.

Table 1
The Number and Subsequent Percentages of TGFs in Relation to Whether They Occur Over Ocean, Coast, or Land

	TGFs	% TGFs	% WWLLN
Ocean	467	36%	32 %
Coast	563	43%	35 %
Land	274	21%	33 %
Total	1,304	100 %	100 %

Note. RHESSI = Reuven Ramaty High Energy Solar Spectroscopic Imager; TGF = terrestrial gamma ray flash; WWLLN = World Wide Lightning Location Network. The third column shows the distribution of all WWLLN detections inside RHESSI's field of view (1,000-km radius from the footpoint), regardless of their association with a TGF or not.

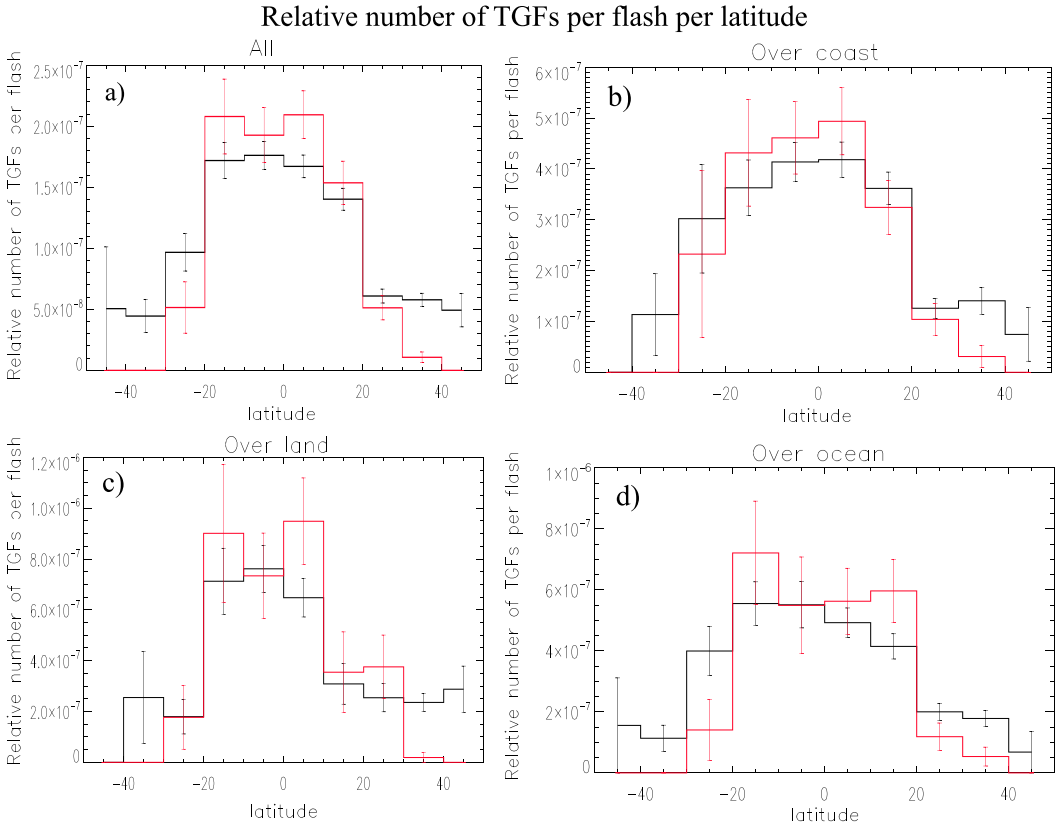

Figure 13. Gjesteland terrestrial gamma ray flashes (TGFs; red) and observationally weak TGFs (black) by latitude. (a) The combined numbers over land, ocean, and coast. (b) Only over the coast, (c) over land, and (d) over ocean.

This raises an interesting question about what the differences are in observationally weak TGFs at lower latitudes and closer to the subsatellite point, compared with the population further out. Imagine if we were to use a "cleaner" set of search parameters, using less than 20° latitude, as well as within 400 km of the subsatellite point. This should represent the subset of weak TGFs that are not dimmed due to their attenuation (from originating far away at a distance) or $1/r^2$ effect but might be intrinsically dimmer or just produced deeper in the atmosphere. This is done in the same way as that in Figure 6, only we use a search radius of 400 km and latitude less than 20°. We find a total of 415 weak TGF events compared to 221 events found by the Gjesteland et al. (2012) algorithm under the same conditions (with WWLLN match). This means that instead of the 1:6 ratio we found earlier, we now only have a 1:2 ratio. This again shows that the majority of weak TGFs are coming from distances further away from the subsatellite point or higher latitudes.

4. Summary

We have shown that by going directly from lightning location data, one can find that there exist TGFs that deposit as little as three counts in the RHESSI detector. Although these cannot be individually identified, once the fluence gets to around 6–7 counts during a 250-μs bin, we can determine a specific event to be a TGF with a fairly good certainty. We find that there could be as many as approximately six times more TGFs inside of RHESSI's FOV that are able to deposit at least three counts in the detector, but too faint in general to be able to be identified as a TGF, and thus determine the location. Comparing the number of observationally weak TGFs to the number of IC flashes in RHESSI's FOV, we find that less than 1% (0.71%) of IC flashes (detected by WWLLN) produce a TGF that deposits three or more counts in RHESSI.

Furthermore, we show that using a power law to fit TGF fluence distribution from RHESSI data might not be appropriate from the start of 2006 and onward, due to the degradation of RHESSI. Even with RHESSI's anneals, which temporarily improve its sensitivity, the general trend is a worsening of the instrument sensitivity. The result is that as WWLLN detection efficiency improves, the RHESSI instrument sensitivity worsens, making it

difficult to compare the population year to year. The result of this is that the fluence distribution gets softened over time (although it periodically improves, but not to its original sensitivity; see Figure 2), which makes any power law fitting to the data unreliable. In addition, any power law exponent that is the result of fitting data from before 2006 is extremely sensitive to the input parameters due to low statistics.

Lastly, we investigate the intrinsically weak TGFs locations in relation to land/coast/ocean. According to previous literature, although WWLLN is biased toward ocean and coastal lightning flashes, the intrinsically weak TGFs and TGFs with WWLLN matches are far more likely to be produced over ocean or coast. This could mean that thunderstorms in these areas are able to develop a higher potential difference before discharging, making it more likely to produce a TGF. This would also explain the discrepancy between TGFs per lightning, as the Congo basin has the highest incidence of lightning flashes, but produces less TGFs per lightning flash.

We also see that observationally weak TGFs are more likely produced at higher (absolute) latitudes compared to those of the Gjesteland et al. (2012) catalog. We believe this is due to the lower altitude of the tropopause (and thus cloud top) and that any TGF produced here will experience more attenuation from the denser atmosphere before reaching the RHESSI instrument. We also find that they tend to be produced further away from the subsatellite point. This means that seemingly a minority of weak TGFs originate from near the subsatellite point at low latitudes.

Acknowledgments
This study was supported by the European Research Council under the European Union's Seventh Framework Programme (FP7/2007-2013)/ERC Grant agreement 320839 and the Research Council of Norway under contracts 208028/F50 and 223252/F50 (CoE). We thank the RHESSI team for the use of RHESSI data and software. We thank the WWLLN team and the institutions contributing to WWLLN. All raw RHESSI data can be downloaded from https://hesperia.gsfc.nasa.gov/rhessi3/. WWLLN data cannot be freely distributed and have to be purchased at http://wwlln.net (however, the specific WWLLN data entries for the TGFs found in this work are included in the supporting information).

References

Abarca, S. F., Corbosiero, K. L., & Galarneau, T. J. (2010). An evaluation of the Worldwide Lightning Location Network (WWLLN) using the National Lightning Detection Network (NLDN) as ground truth. *Journal of Geophysical Research*, *115*, D18206. https://doi.org/10.1029/2009JD013411

Bang, S. D., & Zipser, E. J. (2015). Differences in size spectra of electrified storms over land and ocean. *Geophysical Research Letters*, *42*, 6844–6851. https://doi.org/10.1002/2015GL065264

Boccippio, D. J., Cummins, K. L., Christian, H. J., & Goodman, S. J. (2001). Combined satellite- and surface-based estimation of the intracloud-cloud-to-ground lightning ratio over the continental United States. *Monthly Weather Review*, *129*, 108. https://doi.org/10.1175/1520-0493(2001)129<0108:CSASBE>2.0.CO;2

Briggs, M. S., Fishman, G. J., Connaughton, V., Bhat, P. N., Paciesas, W. S., Preece, R. D., et al. (2010). First results on terrestrial gamma ray flashes from the Fermi Gamma-ray Burst Monitor. *Journal of Geophysical Research*, *115*, A07323. https://doi.org/10.1029/2009JA015242

Briggs, M. S., Xiong, S., Connaughton, V., Tierney, D., Fitzpatrick, G., Foley, S., et al. (2013). Terrestrial gamma-ray flashes in the Fermi era: Improved observations and analysis methods. *Journal of Geophysical Research: Space Physics*, *118*, 3805–3830. https://doi.org/10.1002/jgra.50205

Chen, A. B., Kuo, C.-L., Lee, Y.-J., Su, H.-T., Hsu, R.-R., Chern, J.-L., et al. (2008). Global distributions and occurrence rates of transient luminous events. *Journal of Geophysical Research*, *113*, A08306. https://doi.org/10.1029/2008JA013101

Christian, H. J., Blakeslee, R. J., Boccippio, D. J., Boeck, W. L., Buechler, D. E., Driscoll, K. T., et al. (2003). Global frequency and distribution of lightning as observed from space by the optical transient detector. *Journal of Geophysical Research*, *108*(D1), 4005. https://doi.org/10.1029/2002JD002347

Collier, A. B., Gjesteland, T., & ØStgaard, N. (2011). Assessing the power law distribution of TGFs. *Journal of Geophysical Research*, *116*, A10320. https://doi.org/10.1029/2011JA016612

Connaughton, V., Briggs, M. S., Holzworth, R. H., Hutchins, M. L., Fishman, G. J., Wilson-Hodge, C. A., et al. (2010). Associations between Fermi Gamma-ray Burst Monitor terrestrial gamma ray flashes and sferics from the World Wide Lightning Location Network. *Journal of Geophysical Research*, *115*, A12307. https://doi.org/10.1029/2010JA015681

Connaughton, V., Briggs, M. S., Xiong, S., Dwyer, J. R., Hutchins, M. L., Grove, J. E., et al. (2013). Radio signals from electron beams in terrestrial gamma ray flashes. *Journal of Geophysical Research: Space Physics*, *118*, 2313–2320. https://doi.org/10.1029/2012JA018288

Cooray, V., Jayaratne, R., & Cummins, K. L. (2014). On the peak amplitude of lightning return stroke currents striking the sea. *Atmospheric Research*, *149*, 372–376. https://doi.org/10.1016/j.atmosres.2013.07.012

Dwyer, J. R., & Cummer, S. A. (2013). Radio emissions from terrestrial gamma-ray flashes. *Journal of Geophysical Research: Space Physics*, *118*, 3769–3790. https://doi.org/10.1002/jgra.50188

Dwyer, J. R., & Smith, D. M. (2005). A comparison between Monte Carlo simulations of runaway breakdown and terrestrial gamma-ray flash observations. *Geophysical Research letters*, *32*, L22804. https://doi.org/10.1029/2005GL023848

Dwyer, J. R., Smith, D. M., & Cummer, S. A. (2012). High-Energy Atmospheric physics: Terrestrial Gamma-Ray flashes and related phenomena. *Space Science Reviews*, *173*, 133–196. https://doi.org/10.1007/s11214-012-9894-0

Fishman, G. J., Bhat, P. N., Mallozzi, R., Horack, J. M., Koshut, T., Kouveliotou, C., et al. (1994). Discovery of intense Gamma-Ray flashes of atmospheric origin. *Science*, *264*, 1313–1316. https://doi.org/10.1126/science.264.5163.1313

Fishman, G. J., Briggs, M. S., Connaughton, V., Bhat, P. N., Paciesas, W. S., von Kienlin, A., et al. (2011). Temporal properties of the terrestrial gamma-ray flashes from the Gamma-Ray Burst Monitor on the Fermi Observatory. *Journal of Geophysical Research*, *116*, A07304. https://doi.org/10.1029/2010JA016084

Gjesteland, T., Østgaard, N., Collier, A. B., Carlson, B. E., Eyles, C., & Smith, D. M. (2012). A new method reveals more TGFs in the RHESSI data. *Geophysical Research Letters*, *39*, L05102. https://doi.org/10.1029/2012GL050899

Gjesteland, T., Østgaard, N., Connell, P. H., Stadsnes, J., & Fishman, G. J. (2010). Effects of dead time losses on terrestrial gamma ray flash measurements with the Burst and Transient Source Experiment. *Journal of Geophysical Research*, *115*, A00E21. https://doi.org/10.1029/2009JA014578

Gjesteland, T., Østgaard, N., Laviola, S., Miglietta, M. M., Arnone, E., Marisaldi, M., et al. (2015). Observation of intrinsically bright terrestrial gamma ray flashes from the Mediterranean basin. *Journal of Geophysical Research: Atmospheres*, *120*, 12. https://doi.org/10.1002/2015JD023704

Grefenstette, B. W., Smith, D. M., Dwyer, J. R., & Fishman, G. J. (2008). Time evolution of terrestrial gamma ray flashes. *Geophysical Research Letters*, *35*, L06802. https://doi.org/10.1029/2007GL032922

Grefenstette, B. W., Smith, D. M., Hazelton, B. J., & Lopez, L. I. (2009). First RHESSI terrestrial gamma ray flash catalog. *Journal of Geophysical Research*, *114*, A02314. https://doi.org/10.1029/2008JA013721

Mailyan, B. G., Briggs, M. S., Cramer, E. S., Fitzpatrick, G., Roberts, O. J., Stanbro, M., et al. (2016). The spectroscopy of individual terrestrial gamma-ray flashes: Constraining the source properties. *Journal of Geophysical Research: Space Physics*, *121*, 11,346–11,363. https://doi.org/10.1002/2016JA022702

Mallick, S., Rakov, V., Ngin, T., Gamerota, W., Pilkey, J., Hill, J., et al. (2014). *Evaluation of the WWLLN performance characteristics using rocket-triggered lightning data*. Manaus, Brazil: GROUND/LPE.

Marisaldi, M., Argan, A., Ursi, A., Gjesteland, T., Fuschino, F., Labanti, C., et al. (2015). Enhanced detection of Terrestrial Gamma-Ray Flashes by AGILE. AGU Fall Meeting Abstracts, AE33A-0482.

Marisaldi, M., Fuschino, F., Labanti, C., Galli, M., Longo, F., Del Monte, E., et al. (2010). Detection of terrestrial gamma ray flashes up to 40 MeV by the AGILE satellite. *Journal of Geophysical Research*, *115*, A00E13. https://doi.org/10.1029/2009JA014502

Marisaldi, M., Fuschino, F., Tavani, M., Dietrich, S., Price, C., Galli, M., et al. (2014). Properties of terrestrial gamma ray flashes detected by AGILE MCAL below 30 MeV. *Journal of Geophysical Research: Space Physics*, *119*, 1337–1355. https://doi.org/10.1002/2013JA019301

McTague, L. E., Cummer, S. A., Briggs, M. S., Connaughton, V., Stanbro, M., & Fitzpatrick, G. (2015). A lightning-based search for nearby observationally dim terrestrial gamma ray flashes. *Journal of Geophysical Research: Atmospheres*, *120*, 12,003–12,017. https://doi.org/10.1002/2015JD023475

Mezentsev, A., Østgaard, N., Gjesteland, T., Albrechtsen, K., Lehtinen, N., Marisaldi, M., et al. (2016). Radio emissions from double RHESSI TGFs. *Journal of Geophysical Research: Atmospheres*, *121*, 8006–8022. https://doi.org/10.1002/2016JD025111

Nag, A., & Cummins, K. L. (2017). Negative first stroke leader characteristics in cloud-to-ground lightning over land and ocean. *Geophysical Research Letters*, *44*, 1973–1980. https://doi.org/10.1002/2016GL072270

Nisi, R. S., Østgaard, N., Gjesteland, T., & Collier, A. B. (2014). An altitude and distance correction to the source fluence distribution of TGFs. *Journal of Geophysical Research: Space Physics*, *119*, 8698–8704. https://doi.org/10.1002/2014JA019817

Østgaard, N., Albrechtsen, K. H., Gjesteland, T., & Collier, A. (2015). A new population of terrestrial gamma-ray flashes in the RHESSI data. *Geophysical Research Letters*, *42*, 10,937–10,942. https://doi.org/10.1002/2015GL067064

Østgaard, N., Gjesteland, T., Hansen, R. S., Collier, A. B., & Carlson, B. (2012). The true fluence distribution of terrestrial gamma flashes at satellite altitude. *Journal of Geophysical Research*, *117*, A03327. https://doi.org/10.1029/2011JA017365

Owens, A., Brandenburg, S., Buis, E.-J., Kiewiet, H., Kraft, S., Ostendorf, R. W., et al. (2007). An assessment of radiation damage in space-based germanium detectors due to solar proton events. *Nuclear Instruments and Methods in Physics Research A*, *583*, 285–301. https://doi.org/10.1016/j.nima.2007.07.144

Roberts, O. J., Fitzpatrick, G., Stanbro, M., McBreen, S., Briggs, M. S., Holzworth, R. H., et al. (2018). The First fermi-GBM Terrestrial Gamma Ray Flash Catalog. *Journal of Geophysical Research: Space Physics*, *123*, 4381–4401. https://doi.org/10.1029/2017JA024837

Rudlosky, S. D., & Shea, D. T. (2013). Evaluating WWLLN performance relative to TRMM/LIS. *Geophysical Research Letters*, *40*, 2344–2348. https://doi.org/10.1002/grl.50428

Said, R. K., Cohen, M. B., & Inan, U. S. (2013). Highly intense lightning over the oceans: Estimated peak currents from global GLD360 observations. *Journal of Geophysical Research: Atmospheres*, *118*, 6905–6915. https://doi.org/10.1002/jgrd.50508

Shao, X.-M., Hamlin, T., & Smith, D. M. (2010). A closer examination of terrestrial gamma-ray flash-related lightning processes. *Journal of Geophysical Research*, *115*, A00E30. https://doi.org/10.1029/2009JA014835

Smith, D. M., Buzbee, P., Kelley, N. A., Infanger, A., Holzworth, R. H., & Dwyer, J. R. (2016). The rarity of terrestrial gamma-ray flashes 2: RHESSI stacking analysis. *Journal of Geophysical Research: Atmospheres*, *121*, 11,382–11,404. https://doi.org/10.1002/2016JD025395

Smith, D. M., Dwyer, J. R., Hazelton, B. J., Grefenstette, B. W., Martinez-McKinney, G. F. M., Zhang, Z. Y., et al. (2011). The rarity of terrestrial gamma-ray flashes. *Geophysical Research Letters*, *38*, L08807. https://doi.org/10.1029/2011GL046875

Smith, D. M., Hazelton, B. J., Grefenstette, B. W., Dwyer, J. R., Holzworth, R. H., & Lay, E. H. (2010). Terrestrial gamma ray flashes correlated to storm phase and tropopause height. *Journal of Geophysical Research*, *115*, A00E49. https://doi.org/10.1029/2009JA014853

Smith, D. M., Lin, R. P., Turin, P., Curtis, D. W., Primbsch, J. H., Campbell, R. D., et al. (2002). The RHESSI Spectrometer. *Solar Physics*, *210*, 33–60. https://doi.org/10.1023/A:1022400716414

Splitt, M. E., Lazarus, S. M., Barnes, D., Dwyer, J. R., Rassoul, H. K., Smith, D. M., et al. (2010). Thunderstorm characteristics associated with RHESSI identified terrestrial gamma ray flashes. *Journal of Geophysical Research*, *115*, A00E38. https://doi.org/10.1029/2009JA014622

Tierney, D., Briggs, M. S., Fitzpatrick, G., Chaplin, V. L., Foley, S., McBreen, S., et al. (2013). Fluence distribution of terrestrial gamma ray flashes observed by the Fermi Gamma-ray Burst Monitor. *Journal of Geophysical Research: Space Physics*, *118*, 6644–6650. https://doi.org/10.1002/jgra.50580